# A Dual Hybrid Mode Feedhorn for DSN Antenna Performance Enhancement

R. F. Thomas and D. A. Bathker
Communications Elements Research Section

*A new microwave horn suitable for use in selected DSN antenna feed applications is described. The new horn uses two hybrid modes propagating within corrugated conical waveguide. Expected aperture efficiency improvement, when feeding DSN reflector antennas, as well as bandwidth information is provided. It is concluded that the new horn provides 0.36 dB gain improvement when feeding a symmetrical Cassegrain antenna; it is estimated that 0.29 dB improvement is available when feeding an asymmetric system such as the DSN 64-m antenna tricone configuration. Bandwidth considerations suggest application at X-band (8.4 to 8.5 GHz) is straightforward; the S-band uplink and downlink bands cannot both be covered at this time.*

## I. Introduction

A new microwave horn suitable for use in selected DSN antenna feed applications is described. The new horn uses two hybrid modes propagating within corrugated conical waveguide. Expected aperture efficiency improvement, when feeding DSN reflector antennas is given as well as bandwidth information. It is concluded that the new horn provides 0.36 dB gain improvement when feeding a symmetrical Cassegrain antenna; it is estimated 0.29 dB improvement is available when feeding an asymmetric system such as the DSN 64-m antenna tricone configuration. Bandwidth considerations suggest application at X-band (8.4 to 8.5 GHz) is straightforward; the S-band uplink and downlink bands cannot both be covered at this time.

## II. Previous Work

Prior to 1970, most Deep Space Network (DSN) S-band ground antenna feeds were based on use of two waveguide modes propagating within smooth conical waveguide. Potter (Ref. 1) first described use of the $TE_{11}$ and $TM_{11}$ modes superimposed to obtain superior radiation characteristics in several respects. The higher order TM mode generating required in such a horn is necessarily accomplished at or near the horn throat; due to the length of high gain horns, proper phase synchronism at the horn aperture between the waveguide modes is achieved over a restricted bandwidth (5 to 10%). In the DSN, this previously meant that enhanced horn performance was taken at the downlink (listen) band, while the

uplink (transmit) band had performance equal to or less than single-waveguide-mode horns (Ref. 2).

Work to realize further horn performance (pattern shaping) was only partially successful at that time. Three- and four-mode smooth conical waveguide horns were devised by Ludwig (Ref. 3). The difficulties of controlling mode amplitudes and phases for specific use on DSN antennas were great. It was concluded that only marginal performance was practically available, beyond the two-mode horns.

By 1970, principles described by Minnett and Rumsey (Refs. 4, 5) were applied to feeds for the DSN with excellent results (Ref. 6). This type of horn is based on one hybrid (TE and TM component) mode conducted along a corrugated conical waveguide. The lowest order hybrid mode, $HE_{11}$, used within such a waveguide maintains itself nearly distortion free over a very broad bandwidth, since no phase asynchronism problems arise. In the DSN S-band operations context, it was then possible to provide superior performance over both uplink and downlink frequency bands as well as at the experimental high-power radar frequency. With the advent of very high power (100 to 400 kW, CW) uplink transmitters in the early 1970s, the new wideband horn development was timely in maintaining adequate RF safety performance of the large reflector antennas, through superior feed sidelobe, spillover and aperture illumination characteristics (Ref. 7). The wideband horn was further applied at X- and K-bands for moderate bandwidth radio science applications on the Tricone system of the Goldstone 64-m antenna. Finally, to some degree, such high performance horns allow successful operation of beam waveguide devices such as the Reflex-Dichroic S/X-band Feed (Ref. 8).

In a manner analogous to adding individual TE- and TM-modes within a smooth surface conical waveguide, it is possible to add hybrid modes within a corrugated waveguide (Refs. 9, 10). By so doing, it should be possible to approximate the four-mode horn performance sought after by Ludwig (Ref. 3) using only two hybrid modes. Presumably the problems of maintaining phase synchronism between the modes should be comparable with the two-mode smooth waveguide horn developed by Potter, with comparable bandwidth. Bandwidth should be comparable, since again the higher order mode generator ($HE_{12}$) is located near the horn throat. Nevertheless, some applications do not demand wide bandwidth but would benefit from superior aperture illumination. Thus, development of such a horn was begun at JPL. Potter (Ref. 11), during the course of the experimental work, using Clarricoats' spherical wave technique and his cylindrical hybrid mode equations (Ref. 10), developed a new computer program to calculate radiation patterns of horns employing either smooth or corrugated walls. Although outstanding agreement has been found for smooth dual mode and corrugated single hybrid mode horn patterns (experimental compared to computed), in general the dual hybrid mode horns exhibit less agreement, probably due to additional higher order modes propagating with small amplitude. Nevertheless, the new computer program was a very useful guide in development, and further analytical/experimental comparisons should be made in the future.

## III. Elements of the Dual Hybrid Mode Horn

Figure 1 shows the throat region of the new horn. The $TE_{11}$ input waveguide was constrained to remain the same as previous JPL X-band horns. A center frequency of approximately 8.45 GHz was adopted for development work. The abrupt step, in addition to exciting the $HE_{12}$ mode also plays a major role in controlling the amplitude ratio between the two hybrid modes. The step ratio is finally sized to cut off higher order modes at the upper end of the useable frequency range. The 6° 15′ 15″ half flare angle is the same as existing JPL feedhorns. While somewhat conservative, this moderate flare angle is gradual enough to prevent field distortion at the aperture, for horns with less than 30 dB of gain. Beginning at the interface of Sections 1 and 2 (Fig. 1), the corrugated flare section continues for 109.35 cm (43.050 in.) to an aperture of 31.91 cm (12.563 in.). This aperture size is approximately optimum for the 14.784 deg half-aperture angle of the 64-m antenna with tricone feed subreflector. Corrugations are selected to be $\lambda_0/4$ deep at the center frequency with 5 cycles per freespace wavelength. Although most of the elements of the dual hybrid mode horn influence the impedance bandwidth to a minor degree, the horn is very well matched near the design center frequency, without use of additional elements (Fig. 2). Figure 2 includes all elements shown in Fig. 1. By experiment, the phase center of the new horn is found to be 20 cm (7.88 in.) inside the aperture.

## IV. Performance of the Dual Hybrid Mode Horn

The approach adopted in this reporting is to compare the previously existing horn (single hybrid mode), (Ref. 6), with the new horn, at 8.45 GHz. Bandwidth performance will also be given, using 8.45-GHz dual hybrid mode horn performance as a baseline. Performance for a subreflector

edge angle of 14.784 deg will be given (64-m antenna tricone asymmetric subreflectors). The gain maximum subreflector angle will be noted for possible application to higher noise level systems. Finally, subreflector scattered patterns, at 8.45 GHz only, will be given for the single and dual hybrid mode horns. These patterns will show the improved aperture illumination obtained when using the new horn.

Figure 3 shows E- and H-plane amplitude patterns of the single hybrid and dual hybrid mode feedhorns at the selected center frequency. The efficiencies of these horns, based on horn patterns alone, are given in Table 1. In Table 1, data for the single hybrid mode horn are computed (see Fig. 3 of Ref. 11) rather than measured, while data for the dual hybrid mode horn are measured. This results in a slightly conservative estimate of the improvement. In Table 1, it is seen the dual hybrid mode horn pattern exhibits slightly ($<1\%$) improved spillover efficiency and substantial (5%) improvement in illumination efficiency. Table 2 shows the frequency behavior of the new horn. It is seen that the total efficiency peaks at 8400 MHz; at 8600 MHz the performance is approximately the same as a single hybrid mode horn (Table 1). Figure 4 shows measured E- and H-plane amplitude patterns of the dual hybrid mode horn at the frequency extremes of 8300 and 8600 MHz. For operation over the X-band range 8.40 to 8.50 GHz, the new horn is considered totally adequate.

Figure 5 shows E- and H-plane amplitude patterns of the single and dual hybrid mode horn scattered from a 64-m class antenna subreflector. In this case, to save costs associated with scattering computations from large asymmetric reflectors, we have adopted a symmetric equivalent to the existing 64-m Tricone subreflector (Ref. 12). The scattered patterns show essentially the same forward (polar angle = 165 deg) and rear (polar angle $\simeq$ 65 deg) spillovers; the more uniform amplitude illumination produced by the dual hybrid mode horn is clear.

Table 3 gives the results of efficiency calculations on the two patterns seen in Fig. 5. For the accepted symmetric subreflector case, a performance increase of 0.36 dB is available. It is interesting to note in Table 3, the improved illumination efficiency and the improved central blocking efficiency; the latter is caused by reduced fields in the center portion of the main reflector (Fig. 5). It is estimated, based on Table 1 of Ref. 11, that a loss of 0.07 dB will be incurred if this feed is used in the 64-m tricone asymmetric system, due to energy converted to $m \neq 1$ modes. The net available improvement is therefore +0.29 dB. One uncertainty in estimating the performance improvement of various methods of obtaining more uniform amplitude illumination remains, that of quadripod blocking. With present illumination functions (relatively weaker near the paraboloid periphery) the wider quadripod shadow in that region is of minor consequence. With more uniform illumination, there may be a detrimental side effect. The magnitude of that possible effect is not known.

## V. Summary

A new horn suitable for feeding conventional DSN Cassegrain ground antennas employing parabolic and hyperbolic reflectors has been developed. The new horn offers performance improvements of 0.36 dB in gain for symmetric antennas and an estimated 0.29 dB in gain for the case of the 64-m asymmetric tricone system. Forward and rear spillovers are essentially unchanged from present practice, therefore no noise temperature improvement is realized in the described design. Bandwidth of the new horn is such that it cannot be applied at both DSN S-band uplink (2100 MHz) and downlink (2300 MHz) frequencies simultaneously; it is recommended the new horn be considered for X-band only, in the DSN context. For special S-band low-noise level listen-only applications without transmitter use, the new horn could be applied. The resulting aperture size and overall length will fit a standard feedcone.

## References


1. Potter, P. D., "A New Horn Antenna With Suppressed Sidelobes and Equal Beamwidths," *Microwave Journal*, June 1963.
2. Ludwig, A. C., "Antennas for Space Communication," in *Supporting Research and Advanced Development*, Space Programs Summary 37-33, Vol. IV, pp. 249–255, Jet Propulsion Laboratory, Pasadena, Calif., June 30, 1965.

## References (contd)


3. Ludwig, A. C., "Antennas for Space Communication," in *Supporting Research and Advanced Development*, Space Programs Summary 37-33, Vol. IV, pp. 261–266, June 30, 1965.

4. Minnett, H. C., and Thomas, B., and Mac, A., "A Method of Synthesizing Radiation Patterns With Axial Symmetry," *IEEE Trans. Antennas and Propagation*, pp. 654–656, September 1966.

5. Rumsey, V. H., "Horn Antennas With Uniform Power Patterns Around Their Axes," *IEEE Trans. Antennas and Propagation*, pp. 656-658, September 1966.

6. Brunstein, S. A., "A New Wideband Feedhorn With Equal E- and H-Plane Beamwidths and Suppressed Sidelobes," in *The Deep Space Network*, Space Programs Summary 37-58, Vol. II, pp. 61–64, Jet Propulsion Laboratory, Pasadena, Calif., July 31, 1969.

7. Bathker, D. A., *Predicted and Measured Power Density Description of a Large Ground Microwave System*, Technical Memorandum 33-433, Jet Propulsion Laboratory, Pasadena, Calif., April 15, 1971.

8. Bathker, D. A., "Dual Frequency Dichroic Feed Performance," presented at AGARD Antennas for Avionics Panel, Munich, Germany, November 26–29, 1973.

9. Thomas, B., and Mac, A., "Theoretical Performance of Prime-Forms Paraboloids Using Cylindrical Hybrid-Mode Feeds," *Proc. IEEE*, Vol. 118, No. 11, November 1971.

10. Clarricoats, P. J. B., and Saha, P. K., "Propagation and Radiation Behavior of Corrugated Feeds, Parts I and II," *Proc. IEEE*, Vol. 118, No. 9, September 1971.

11. Potter, P. D., "A New Computer Program for the Design and Analysis of High Performance Conical Feedhorns," in *The Deep Space Network*, Technical Report 32-1526, Vol. XIII, pp. 92–107, Jet Propulsion Laboratory, Pasadena, Calif., February 15, 1973.

12. Potter, P. D., "Shaped Antenna Designs and Performance for 64-m Class DSN Antennas," in *The Deep Space Network Progress Report 42-20*, pp. 92–111, Jet Propulsion Laboratory, Pasadena, Calif., April 15, 1974.

**Table 1. Single hybrid mode and dual hybrid mode horn efficiencies 8450 MHz**

| Efficiencies at $\theta$ = 14.784 deg | Single hybrid-mode horn | Dual hybrid-mode horn |
|---|---|---|
| Spillover $\eta_S$ | 0.9483 | 0.9554 |
| Illumination $\eta_I$ | 0.8443 | 0.8989 |
| Cross-polarization $\eta_X$ | 0.9999 | 0.9999 |
| Phase $\eta_P$ | 0.9983 | 0.9926 |
| TOTAL $\eta_T$ | 0.7993 | 0.8523 |
| Maximum efficiency $\eta_{MAX}$ | 0.8153 at $\theta$ = 13.293 deg | 0.8646 at $\theta$ = 13.784 deg |

**Table 2. Dual hybrid mode horn efficiencies as a function of frequency at $\theta$ = 14.784 deg**

| Frequency, MHz | $\eta_S$ | $\eta_I$ | $\eta_X$ | $\eta_P$ | $\eta_T$ TOTAL | $\eta_{MAX}$ |
|---|---|---|---|---|---|---|
| 8300 | 0.9385 | 0.9437 | 0.9961 | 0.9704 | 0.8496 | 0.8502 @ $\theta$ = 14.563 deg |
| 8400 | 0.9506 | 0.9137 | 0.9998 | 0.9922 | 0.8616 | 0.8685 @ $\theta$ = 14.000 deg |
| 8450 | 0.9554 | 0.8989 | 0.9999 | 0.9926 | 0.8523 | 0.8646 @ $\theta$ = 13.784 deg |
| 8500 | 0.9593 | 0.8849 | 0.9993 | 0.9879 | 0.8380 | 0.8558 @ $\theta$ = 13.501 deg |
| 8600 | 0.9664 | 0.8523 | 0.9969 | 0.9630 | 0.7906 | 0.8245 @ $\theta$ = 12.937 deg |

**Table 3. Subreflector scattered pattern efficiencies, 8450 MHz (tricone symmetric equivalent subreflector)**

| Efficiencies at 61.104 deg | Single hybrid-mode feed | Dual hybrid-mode feed | Dual hybrid mode improvement, dB |
|---|---|---|---|
| Spillover $\eta_S$ | 0.9447 | 0.9529 | +0.037 |
| Illumination $\eta_I$ | 0.8474 | 0.9008 | +0.266 |
| Cross-polarization $\eta_X$ | 0.9999 | 0.9999 | 0 |
| Phase $\eta_P$ | 0.9718 | 0.9670 | −0.021 |
| Blocking $\eta_B$ | 0.9441 | 0.9616 | +0.080 |
| TOTAL $\eta_T$ | 0.7344 | 0.7981 | +3.361 |

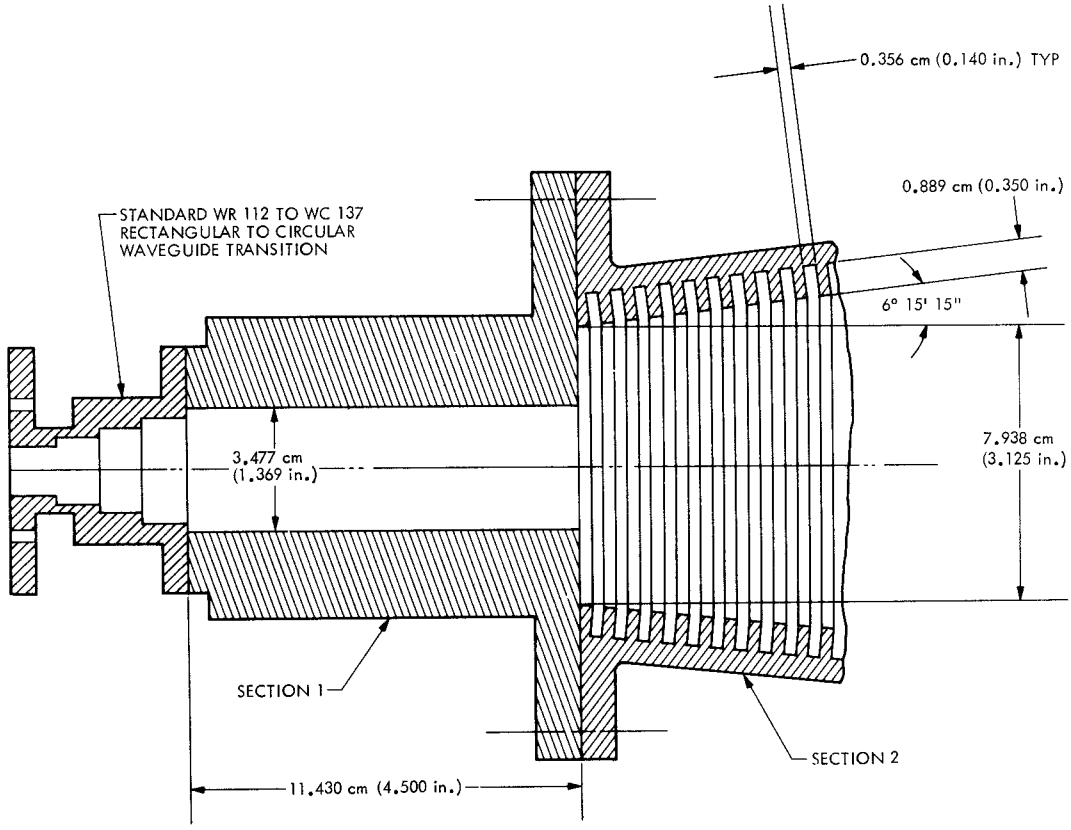


**Fig. 1. Throat region of dual hybrid mode horn**

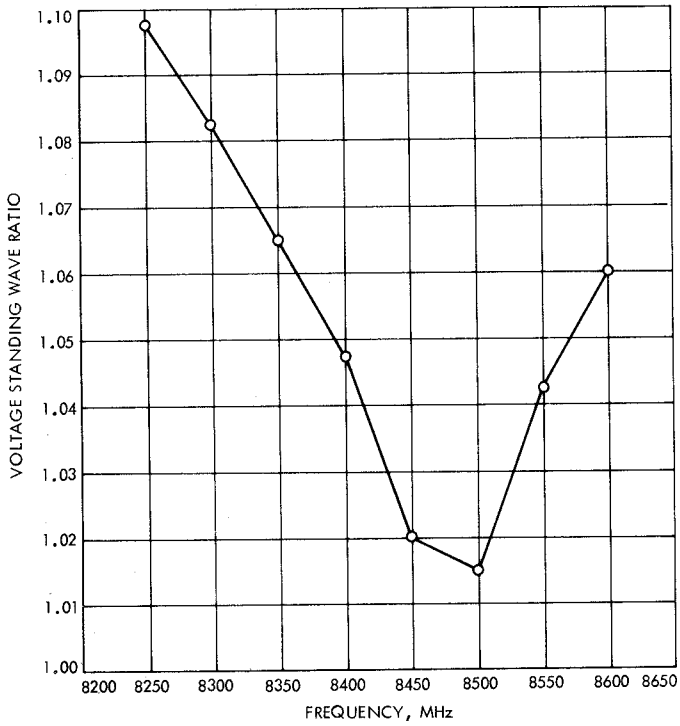


**Fig. 2. Impedance bandwidth of dual hybrid mode horn**

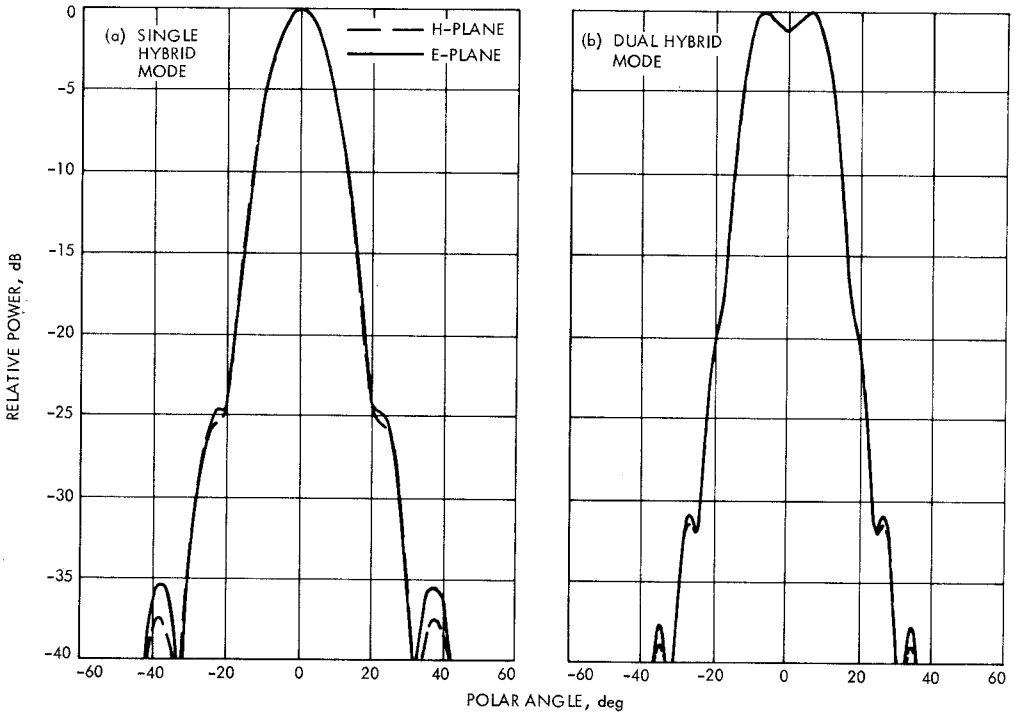


**Fig. 3. Feedhorn amplitude patterns, 8.45 GHz**

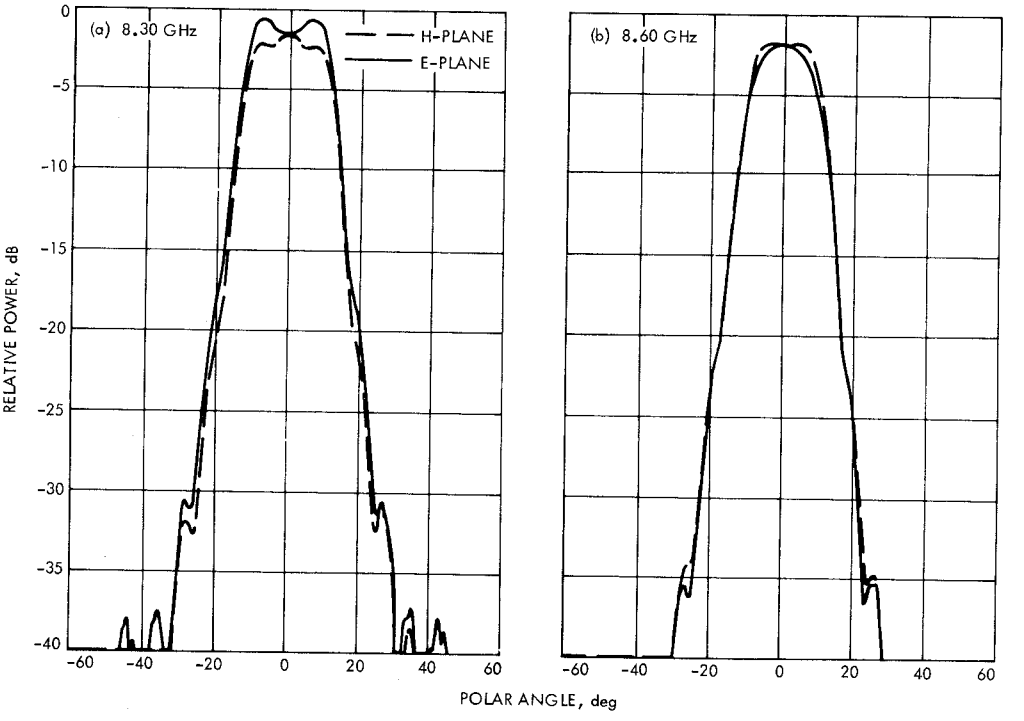


**Fig. 4. Dual hybrid mode feedhorn amplitude patterns, 8.30 and 8.60 GHz**

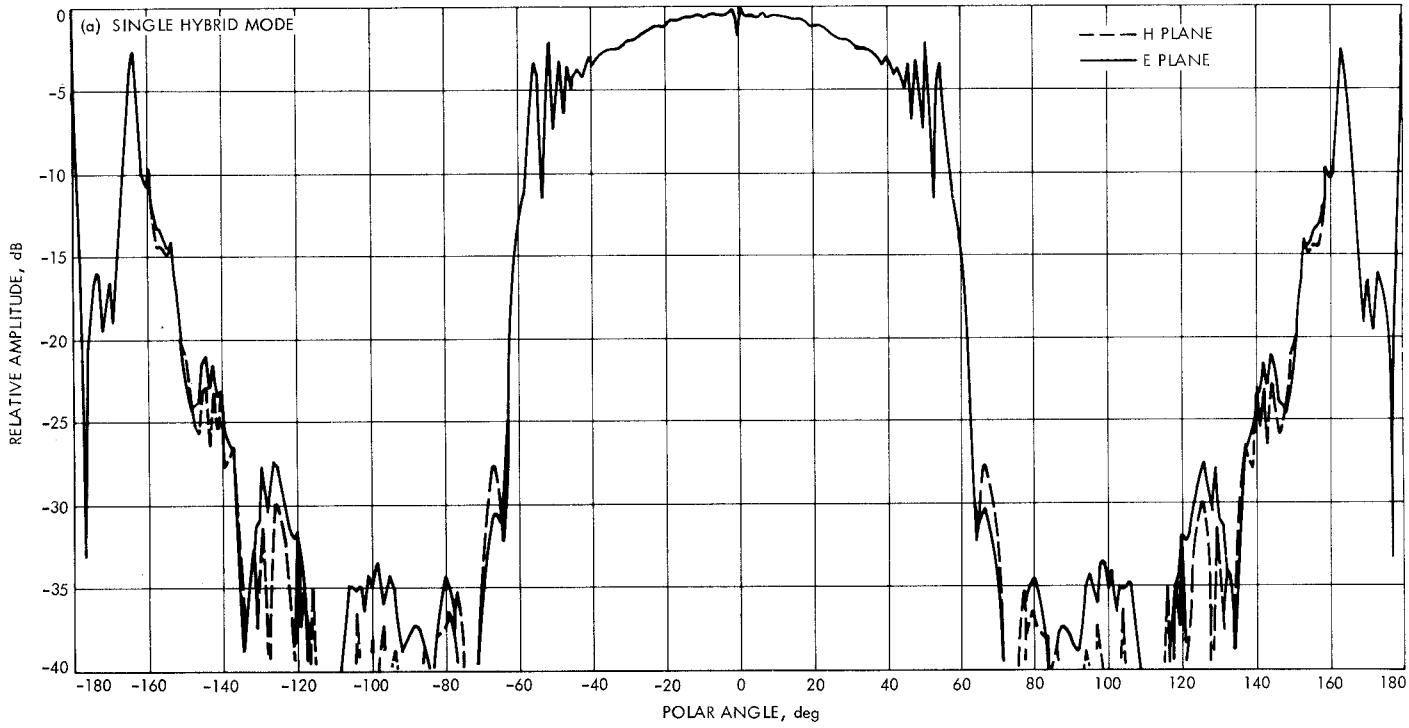


**Fig. 5. Symmetric subreflector amplitude patterns, 8.45 GHz**

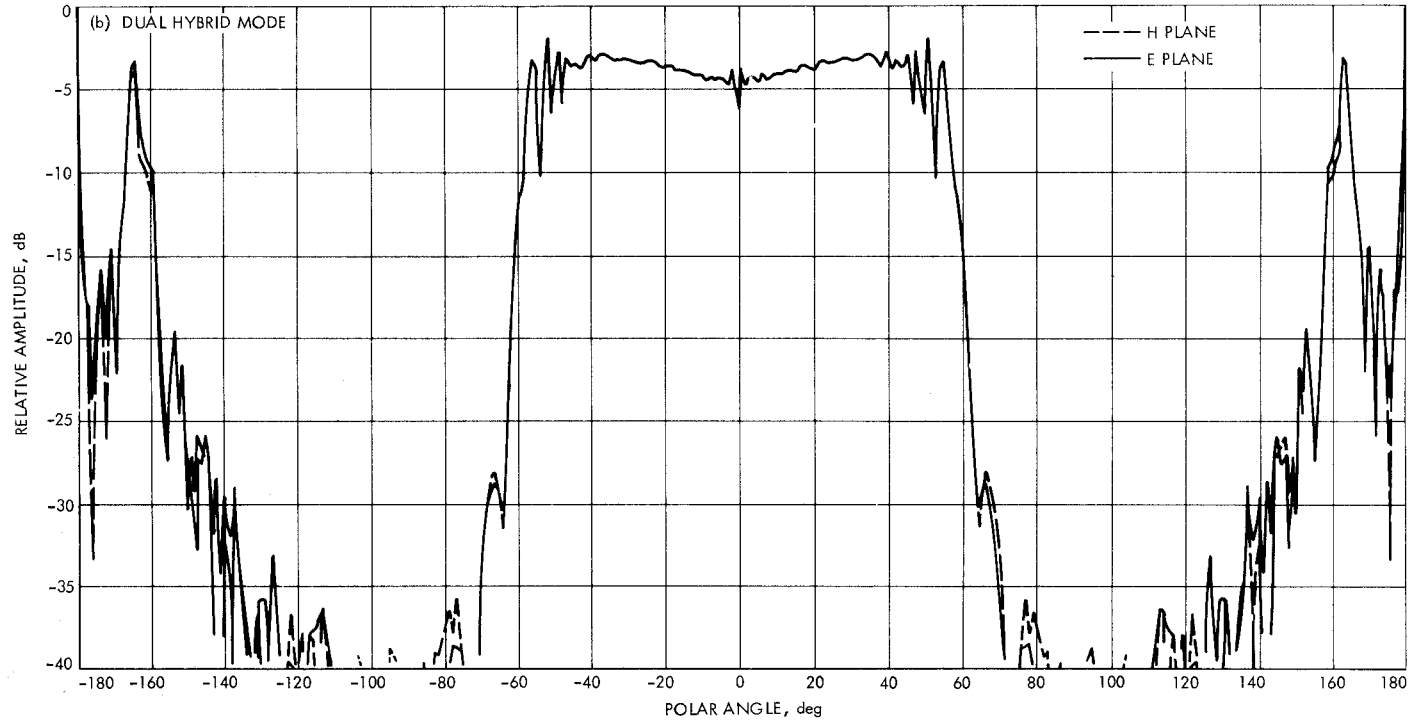


**Fig. 5 (contd)**